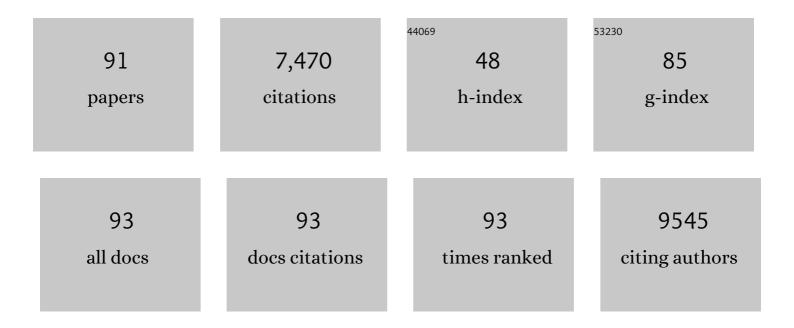
List of Publications by Year in descending order

Source: https://exaly.com/author-pdf/6949378/publications.pdf Version: 2024-02-01



#	Article	IF	CITATIONS
1	Spatial Characterization of Tumor Perfusion Properties from 3D DCE-US Perfusion Maps are Early Predictors of Cancer Treatment Response. Scientific Reports, 2020, 10, 6996.	3.3	9
2	Evaluation of integrin αvβ6 cystine knot PET tracers to detect cancer and idiopathic pulmonary fibrosis. Nature Communications, 2019, 10, 4673.	12.8	73
3	Point Shear Wave Elastography Using Machine Learning to Differentiate Renal Cell Carcinoma and Angiomyolipoma. Ultrasound in Medicine and Biology, 2019, 45, 1944-1954.	1.5	10
4	Multimodality Hyperpolarized C-13 MRS/PET/Multiparametric MR Imaging for Detection and Image-Guided Biopsy of Prostate Cancer: First Experience in a Canine Prostate Cancer Model. Molecular Imaging and Biology, 2019, 21, 861-870.	2.6	6
5	Quantitative Ultrasound Spectroscopy for Differentiation of Hepatocellular Carcinoma from At-Risk and Normal Liver Parenchyma. Clinical Cancer Research, 2019, 25, 6683-6691.	7.0	8
6	Pharmacokinetic Modeling of Targeted Ultrasound Contrast Agents for Quantitative Assessment of Anti-Angiogenic Therapy: a Longitudinal Case-Control Study in Colon Cancer. Molecular Imaging and Biology, 2019, 21, 633-643.	2.6	9
7	A multiâ€model framework to estimate perfusion parameters using contrastâ€enhanced ultrasound imaging. Medical Physics, 2019, 46, 590-600.	3.0	5
8	How to perform Contrast-Enhanced Ultrasound (CEUS). Ultrasound International Open, 2018, 04, E2-E15.	0.6	222
9	Thy1-Targeted Microbubbles for Ultrasound Molecular Imaging of Pancreatic Ductal Adenocarcinoma. Clinical Cancer Research, 2018, 24, 1574-1585.	7.0	32
10	Intraoperative Resection Guidance with Photoacoustic and Fluorescence Molecular Imaging Using an Anti–B7-H3 Antibody-Indocyanine Green Dual Contrast Agent. Clinical Cancer Research, 2018, 24, 3572-3582.	7.0	33
11	Anatomical Road Mapping Using CT and MR Enterography for Ultrasound Molecular Imaging of Small Bowel Inflammation in Swine. European Radiology, 2018, 28, 2068-2076.	4.5	1
12	Point Shear Wave Elastography for Grading Liver Fibrosis: Can the Number of Measurements Be Reduced?. Ultrasound in Medicine and Biology, 2018, 44, 2569-2577.	1.5	1
13	Ultrasound-guided delivery of thymidine kinase–nitroreductase dual therapeutic genes by PECylated-PLGA/PEI nanoparticles for enhanced triple negative breast cancer therapy. Nanomedicine, 2018, 13, 1051-1066.	3.3	33
14	US Molecular Imaging of Acute Ileitis: Anti-Inflammatory Treatment Response Monitored with Targeted Microbubbles in a Preclinical Model. Radiology, 2018, 289, 90-100.	7.3	9
15	Contrast-enhanced ultrasound of malignant liver lesions. Abdominal Radiology, 2018, 43, 819-847.	2.1	57
16	Molecular Contrast-Enhanced Ultrasound Imaging of Radiation-Induced P-Selectin Expression in Healthy Mice Colon. International Journal of Radiation Oncology Biology Physics, 2017, 97, 581-585.	0.8	9
17	Reduced dose CT with model-based iterative reconstruction compared to standard dose CT of the chest, abdomen, and pelvis in oncology patients: intra-individual comparison study on image quality and lesion conspicuity. Abdominal Radiology, 2017, 42, 2279-2288.	2.1	23
18	American College of Radiology Contrast Enhanced Ultrasound Liver Imaging Reporting and Data System (CEUS LI-RADS) for the diagnosis of Hepatocellular Carcinoma: a pictorial essay. Ultraschall in Der Medizin, 2017, 38, 320-324.	1.5	84

#	Article	IF	CITATIONS
19	Contrast Enhanced Ultrasound (CEUS) Liver Imaging Reporting and Data System (LI-RADS®): the official version by the American College of Radiology (ACR). Ultraschall in Der Medizin, 2017, 38, 85-86.	1.5	110
20	Intra-Individual Comparison between 2-D Shear Wave Elastography (GE System) and Virtual Touch Tissue Quantification (Siemens System) in Grading Liver Fibrosis. Ultrasound in Medicine and Biology, 2017, 43, 2774-2782.	1.5	14
21	Early prediction of tumor response to bevacizumab treatment in murine colon cancer models using three-dimensional dynamic contrast-enhanced ultrasound imaging. Angiogenesis, 2017, 20, 547-555.	7.2	26
22	Intra-Animal Comparison between Three-dimensional Molecularly Targeted US and Three-dimensional Dynamic Contrast-enhanced US for Early Antiangiogenic Treatment Assessment in Colon Cancer. Radiology, 2017, 282, 443-452.	7.3	25
23	Quantitative Three-Dimensional Dynamic Contrast-Enhanced Ultrasound Imaging: First-In-Human Pilot Study in Patients with Liver Metastases. Theranostics, 2017, 7, 3745-3758.	10.0	35
24	Spectroscopic Photoacoustic Molecular Imaging of Breast Cancer using a B7-H3-targeted ICG Contrast Agent. Theranostics, 2017, 7, 1463-1476.	10.0	56
25	Ultrasound-guided drug delivery in cancer. Ultrasonography, 2017, 36, 171-184.	2.3	143
26	Ultrasound Molecular Imaging With BR55 in Patients With Breast and Ovarian Lesions: First-in-Human Results. Journal of Clinical Oncology, 2017, 35, 2133-2140.	1.6	178
27	Ultrasound Molecular Imaging of the Breast Cancer Neovasculature using Engineered Fibronectin Scaffold Ligands: A Novel Class of Targeted Contrast Ultrasound Agent. Theranostics, 2016, 6, 1740-1752.	10.0	38
28	VEGFR2-Targeted Three-Dimensional Ultrasound Imaging Can Predict Responses to Antiangiogenic Therapy in Preclinical Models of Colon Cancer. Cancer Research, 2016, 76, 4081-4089.	0.9	38
29	Ultrasound-guided therapeutic modulation of hepatocellular carcinoma using complementary microRNAs. Journal of Controlled Release, 2016, 238, 272-280.	9.9	62
30	Photoacoustic Imaging in Oncology: Translational Preclinical and Early Clinical Experience. Radiology, 2016, 280, 332-349.	7.3	153
31	Multimodality Molecular Imaging of Cardiac Cell Transplantation: Part I. Reporter Gene Design, Characterization, and Optical in Vivo Imaging of Bone Marrow Stromal Cells after Myocardial Infarction. Radiology, 2016, 280, 815-825.	7.3	12
32	Multimodality Molecular Imaging of Cardiac Cell Transplantation: Part II. In Vivo Imaging of Bone Marrow Stromal Cells in Swine with PET/CT and MR Imaging. Radiology, 2016, 280, 826-836.	7.3	12
33	Sonoporation: Applications for Cancer Therapy. Advances in Experimental Medicine and Biology, 2016, 880, 263-291.	1.6	43
34	Clinical photoacoustic imaging of cancer. Ultrasonography, 2016, 35, 267-280.	2.3	123
35	Three-Dimensional Ultrasound Molecular Imaging of Angiogenesis in Colon Cancer Using a Clinical Matrix Array Ultrasound Transducer. Investigative Radiology, 2015, 50, 322-329.	6.2	43
36	Assessment of Inflammation in an Acute on Chronic Model of Inflammatory Bowel Disease with Ultrasound Molecular Imaging. Theranostics, 2015, 5, 1175-1186.	10.0	36

#	Article	IF	CITATIONS
37	Vascular Endothelial Growth Factor Receptor Type 2–targeted Contrast-enhanced US of Pancreatic Cancer Neovasculature in a Genetically Engineered Mouse Model: Potential for Earlier Detection. Radiology, 2015, 274, 790-799.	7.3	59
38	Ultrasound molecular imaging: Moving toward clinical translation. European Journal of Radiology, 2015, 84, 1685-1693.	2.6	168
39	Polymer Nanoparticles Mediated Codelivery of AntimiR-10b and AntimiR-21 for Achieving Triple Negative Breast Cancer Therapy. ACS Nano, 2015, 9, 2290-2302.	14.6	221
40	Ultrasound-guided delivery of microRNA loaded nanoparticles into cancer. Journal of Controlled Release, 2015, 203, 99-108.	9.9	128
41	Breast Cancer Detection by B7-H3–Targeted Ultrasound Molecular Imaging. Cancer Research, 2015, 75, 2501-2509.	0.9	90
42	Three-dimensional Dynamic Contrast-enhanced US Imaging for Early Antiangiogenic Treatment Assessment in a Mouse Colon Cancer Model. Radiology, 2015, 277, 424-434.	7.3	32
43	Quantitative Assessment of Inflammation in a Porcine Acute Terminal Ileitis Model: US with a Molecularly Targeted Contrast Agent. Radiology, 2015, 276, 809-817.	7.3	29
44	Combining in Vitro Diagnostics with in Vivo Imaging for Earlier Detection of Pancreatic Ductal Adenocarcinoma: Challenges and Solutions. Radiology, 2015, 277, 644-661.	7.3	23
45	Multiparametric Spectroscopic Photoacoustic Imaging of Breast Cancer Development in a Transgenic Mouse Model. Theranostics, 2014, 4, 1062-1071.	10.0	44
46	Stromal response to Hedgehog signaling restrains pancreatic cancer progression. Proceedings of the National Academy of Sciences of the United States of America, 2014, 111, E3091-100.	7.1	421
47	CT Perfusion of the Liver: Principles and Applications in Oncology. Radiology, 2014, 272, 322-344.	7.3	154
48	Ultrasound Molecular Imaging in a Human CD276 Expression–Modulated Murine Ovarian Cancer Model. Clinical Cancer Research, 2014, 20, 1313-1322.	7.0	39
49	Ultrasound and Microbubble Guided Drug Delivery: Mechanistic Understanding and Clinical Implications. Current Pharmaceutical Biotechnology, 2014, 14, 743-752.	1.6	113
50	Detection of Pancreatic Ductal Adenocarcinoma in Mice by Ultrasound Imaging of Thymocyte Differentiation Antigen 1. Gastroenterology, 2013, 145, 885-894.e3.	1.3	63
51	New Technologies in Clinical Ultrasound. Seminars in Roentgenology, 2013, 48, 214-223.	0.6	31
52	Ultrasound and Microbubble–Mediated Gene Delivery in Cancer. Investigative Radiology, 2013, 48, 755-769.	6.2	36
53	Molecular Imaging of Inflammation in Inflammatory Bowel Disease with a Clinically Translatable Dual-Selectin–targeted US Contrast Agent: Comparison with FDG PET/CT in a Mouse Model. Radiology, 2013, 267, 818-829.	7.3	60
54	Acoustic and Photoacoustic Molecular Imaging of Cancer. Journal of Nuclear Medicine, 2013, 54, 1851-1854.	5.0	92

#	Article	IF	CITATIONS
55	Earlier Detection of Breast Cancer with Ultrasound Molecular Imaging in a Transgenic Mouse Model. Cancer Research, 2013, 73, 1689-1698.	0.9	85
56	Quantification and Monitoring of Inflammation in Murine Inflammatory Bowel Disease with Targeted Contrast-enhanced US. Radiology, 2012, 262, 172-180.	7.3	71
57	Cationic versus Neutral Microbubbles for Ultrasound-mediated Gene Delivery in Cancer. Radiology, 2012, 264, 721-732.	7.3	99
58	Pharmacokinetically Stabilized Cystine Knot Peptides That Bind Alpha-v-Beta-6 Integrin with Single-Digit Nanomolar Affinities for Detection of Pancreatic Cancer. Clinical Cancer Research, 2012, 18, 839-849.	7.0	95
59	Molecular Body Imaging: MR Imaging, CT, and US. Part I. Principles. Radiology, 2012, 263, 633-643.	7.3	193
60	Antiangiogenic and Radiation Therapy. Investigative Radiology, 2012, 47, 25-32.	6.2	40
61	Ultrasound Molecular Imaging Contrast Agent Binding to Both E- and P-Selectin in Different Species. Investigative Radiology, 2012, 47, 516-523.	6.2	52
62	Quantitative assessment of tumor angiogenesis using real-time motion-compensated contrast-enhanced ultrasound imaging. Angiogenesis, 2012, 15, 433-442.	7.2	26
63	β-Catenin Regulates Hepatic Mitochondrial Function and Energy Balance in Mice. Gastroenterology, 2012, 143, 754-764.	1.3	79
64	Stromal galectin-1 expression is associated with long-term survival in resectable pancreatic ductal adenocarcinoma. Cancer Biology and Therapy, 2012, 13, 899-907.	3.4	56
65	Ultrasound-Mediated Gene Delivery with Cationic Versus Neutral Microbubbles: Effect of DNA and Microbubble Dose on <i>In Vivo</i> Transfection Efficiency. Theranostics, 2012, 2, 1078-1091.	10.0	83
66	Molecular Body Imaging: MR Imaging, CT, and US. Part II. Applications. Radiology, 2012, 264, 349-368.	7.3	61
67	Adenocarcinoma of the uncinate process of the pancreas: MDCT patterns of local invasion and clinical features at presentation. European Radiology, 2012, 22, 1067-1074.	4.5	31
68	Incidentally discovered solid pancreatic masses: imaging and clinical observations. Abdominal Imaging, 2012, 37, 91-97.	2.0	23
69	Targeted Contrast-Enhanced Ultrasound: An Emerging Technology in Abdominal and Pelvic Imaging. Gastroenterology, 2011, , .	1.3	0
70	Targeted Contrast-Enhanced Ultrasound: An Emerging Technology in Abdominal and Pelvic Imaging. Gastroenterology, 2011, 140, 785-790.e6.	1.3	54
71	Assessment and Monitoring Tumor Vascularity With Contrast-Enhanced Ultrasound Maximum Intensity Persistence Imaging. Investigative Radiology, 2011, 46, 187-195.	6.2	56
72	Early Diagnosis of Ovarian Carcinoma: Is a Solution in Sight?. Radiology, 2011, 259, 329-345.	7.3	82

#	Article	IF	CITATIONS
73	Tumor Angiogenic Marker Expression Levels during Tumor Growth: Longitudinal Assessment with Molecularly Targeted Microbubbles and US Imaging. Radiology, 2011, 258, 804-811.	7.3	123
74	Molecular ultrasound assessment of tumor angiogenesis. Angiogenesis, 2010, 13, 175-188.	7.2	79
75	Antioxidants Improve Early Survival of Cardiomyoblasts After Transplantation to the Myocardium. Molecular Imaging and Biology, 2010, 12, 325-334.	2.6	26
76	Targeted Contrast-Enhanced Ultrasound Imaging of Tumor Angiogenesis with Contrast Microbubbles Conjugated to Integrin-Binding Knottin Peptides. Journal of Nuclear Medicine, 2010, 51, 433-440.	5.0	156
77	Antiangiogenic Cancer Therapy: Monitoring with Molecular US and a Clinically Translatable Contrast Agent (BR55). Radiology, 2010, 256, 519-527.	7.3	158
78	Pathways of Extrapancreatic Perineural Invasion by Pancreatic Adenocarcinoma: Evaluation With 3D Volume-Rendered MDCT Imaging. American Journal of Roentgenology, 2010, 194, 668-674.	2.2	61
79	Focal Liver Lesions: Detection and Characterization at Double-Contrast Liver MR Imaging with Ferucarbotran and Gadobutrol versus Single-Contrast Liver MR Imaging. Radiology, 2009, 253, 724-733.	7.3	23
80	Evaluation of Periampullary Pathology With CT Volumetric Oblique Coronal Reformations. American Journal of Roentgenology, 2009, 193, W202-W208.	2.2	24
81	Imaging Gene Expression in Human Mesenchymal Stem Cells: From Small to Large Animals. Radiology, 2009, 252, 117-127.	7.3	83
82	Comparison of Optical Bioluminescence Reporter Gene and Superparamagnetic Iron Oxide MR Contrast Agent as Cell Markers for Noninvasive Imaging of Cardiac Cell Transplantation. Molecular Imaging and Biology, 2009, 11, 178-187.	2.6	84
83	MR angiography with parallel acquisition for assessment of the visceral arteries: comparison with conventional MR angiography and 64-detector-row computed tomography. European Radiology, 2009, 19, 2679-2688.	4.5	3
84	Molecular imaging in drug development. Nature Reviews Drug Discovery, 2008, 7, 591-607.	46.4	1,000
85	Reporter Gene Imaging Following Percutaneous Delivery in Swine. Journal of the American College of Cardiology, 2008, 51, 595-597.	2.8	20
86	US Imaging of Tumor Angiogenesis with Microbubbles Targeted to Vascular Endothelial Growth Factor Receptor Type 2 in Mice. Radiology, 2008, 246, 508-518.	7.3	293
87	Monitoring of the Biological Response to Murine Hindlimb Ischemia With ⁶⁴ Cu-Labeled Vascular Endothelial Growth Factor-121 Positron Emission Tomography. Circulation, 2008, 117, 915-922.	1.6	69
88	Imaging of VEGF Receptor in a Rat Myocardial Infarction Model Using PET. Journal of Nuclear Medicine, 2008, 49, 667-673.	5.0	102
89	Targeted Microbubbles for Imaging Tumor Angiogenesis: Assessment of Whole-Body Biodistribution with Dynamic Micro-PET in Mice. Radiology, 2008, 249, 212-219.	7.3	175
90	Dual-targeted Contrast Agent for US Assessment of Tumor Angiogenesis in Vivo. Radiology, 2008, 248, 936-944.	7.3	206

#	Article	IF	CITATIONS
91	Recurrent Lower-Limb Varicose Veins: Effect of Direct Contrast-enhanced Three-dimensional MR Venographic Findings on Diagnostic Thinking and Therapeutic Decisions. Radiology, 2008, 247, 887-895.	7.3	15